

Five-phase induction motor drive for weak and remote grid system

¹Shaikh Moinoddin, ²Atif Iqbal* and ³Elmahdi M. Elsherif

^{1,3} Department of Electronics & Computer Engineering, Sebha University, Sebha, LIBYA

²*Department of Electrical Engineering, Aligarh Muslim University, Aligarh, INDIA

*Corresponding Author (e-mail: atif_iqbal1@rediffmail.com, Atif Iqbal; Tel. +919411210372)

Abstract

Multi-phase (more than three-phase) motor drive systems have attracted much attention in recent years due to some inherent advantages which they offer when compared to the three-phase counterpart. Presently the grid power available is only limited to three-phase so the supply to multi-phase motors is invariably given from power electronic converters. Thus the paper focuses on the inverter controlled five-phase induction motor drive system for variable speed applications. The paper presents inverter control method for five-phase variable speed induction motor drives. The proposed solution may be employed in the applications not requiring very precise position and speed control such as water pumping especially in weak grid system with poor power quality. The inverter is operated in different operating modes with conduction angle varying from 180° to 108° conduction modes and the performance is evaluated in terms of the harmonic contents in the output phase voltages. It is shown that optimum performance is achieved by operating inverter at 144° conduction mode. Experimental and analytical results are included in the paper.

Keywords: Voltage source inverter, ten-step operation, conduction modes, power grid, Induction motor drive

1. Introduction

Variable speed electric drives predominately utilise three-phase machines. However, since the variable speed ac drives require a power electronic converter for their supply (in vast majority of cases an inverter with a dc link), the number of machine phases is essentially not limited. This has led to an increase in the interest in multi-phase ac drive applications, since multi-phase machines offer some inherent advantages over their three-phase counterpart. Interesting research results have been published over the years on multi-phase drives and detailed review is available in Singh (2002), Jones and Levi (2002), Bojoi *et al.* (2006), Levi *et al.* (2007), Levi (2008a) and Levi (2008b). Major advantages of using a multi-phase machine instead of a three-phase machine are higher torque density, greater efficiency, reduced torque pulsations, greater fault tolerance, and reduction in the required rating per inverter leg (and therefore simpler and more reliable power conditioning equipment). Noise characteristics of multi-phase drives are better when compared three-phase drive as demonstrated by Hodge *et al.* (2002) and Golubev and Ignatenko (2000). Higher Phase number yield smoother torque due to the simultaneous increase of the frequency of the torque pulsation and reduction of the torque ripple magnitude, as presented by Williamson and Smith (2006) and Apsley (2006).

Higher torque density in a multi-phase machine is possible because fundamental spatial field harmonic and space harmonic fields can be used to enhance total torque as presented by Xu *et al.* (2001a) and Xu *et al.* (2001b), Shi *et al.* (2001), Lyra and Lipo (2002), Duran *et al.* (2008) and Arahall and Duran (2009). This advantage of enhanced torque production stems from the fact that vector control of the machine's flux and torque, produced by the interaction of the fundamental field component and the fundamental stator current component, requires only two stator currents (*d-q* current components). In a multi-phase machine, with at least five phases or more, there are therefore additional degrees of freedom, which can be utilised to enhance the torque production through injection of higher order current harmonics. The stability analysis of five-phase drive system for harmonic injection scheme is carried out by Duran *et al.* (2008) for both concentrated winding and distributed winding machines. It was concluded that the 3rd harmonic injection not only enhances the torque production but also offers a more stable control structure.

The studies on multi-phase drive system carried out so far is for high performance variable speed applications. Multi-phase drive is seen as a serious contender for niche applications such as ship propulsion, traction, electric vehicles and in safety critical

applications requiring high degree of redundancy. However, general purpose drive applications using multi-phase machines are not yet investigated in detail. This paper advocates the use of a five-phase drive system for general purpose applications such as water pumping in remote and weak grid locations where the power quality is not adequate for operating sophisticated microprocessor based controllers due to their stringent power quality requirements. Further, the costs of such high performance drive systems are too high to be borne by poor farmers in remote locations. The question then arises why five-phase drive is at all required not conventional three-phase drive. The answer lies in the fault tolerant characteristic, reliable and higher efficiency of five-phase drive compared to three-phase drive (detailed by Apsley et al. (2006), Arhal and Duran (2008)). The power electronic converters supplying multi-phase drives are controlled using advanced digital signal processors (DSP) and Field programmable Gate Arrays (FPGA). Many modulation techniques implemented using DSPs and FPGAs are proposed in the literature for controlling the multi-phase power electronic converters, Iqbal and Levi (2005). In contrast this paper proposes simple, reliable and cheap controller circuit using analogue components and square wave operation of a five-phase voltage source inverter (VSI). In environment of weak grid with poor power quality, stepped operation of voltage source inverter may be considered as more viable solution in comparison to PWM mode. This paper thus analyses the performance of a five-phase induction motor drive supplied by a five-phase VSI operating in square wave mode. Conduction angle is varied from 180° leading to ten-step operation to 108°. A detailed comparison of inverter performance on various conduction angles is elaborated. It will be shown that a trade off exist between the fundamental output voltage and their harmonic content. Analytical, simulation and experimental results are provided.

The paper is organised in ten different sections; first section details the literature review and laid down the need of the proposed drive topology, modelling of a five-phase VSI is illustrated in the second section, third section elaborates the proposed five-phase induction motor drive structure. Fourth section describes the gate drive circuit for the five-phase VSI and fifth section discusses the experimental results obtained for testing of the fabricated inverter, the analysis of results, and compares the magnitude of torque pulsation in a three-phase and a five-phase drive system then sixth section concludes the finding followed by the references.

2. Modelling of a five-phase VSI-review

Power circuit topology of a five-phase VSI, is shown in Figure 1. Each switch in the circuit consists of two power semiconductor devices, connected in anti-parallel. One of these is a fully controllable semiconductor, such as a bipolar transistor or IGBT, while the second one is a diode. The input of the inverter is a dc voltage, which is regarded further on as being constant. The inverter outputs are denoted in Figure 1 with lower case letters (a,b,c,d,e), while the points of connection of the outputs to inverter legs have symbols in capital letters (A,B,C,D,E), The shift between each phase voltage is $(360/5)=72^\circ$.

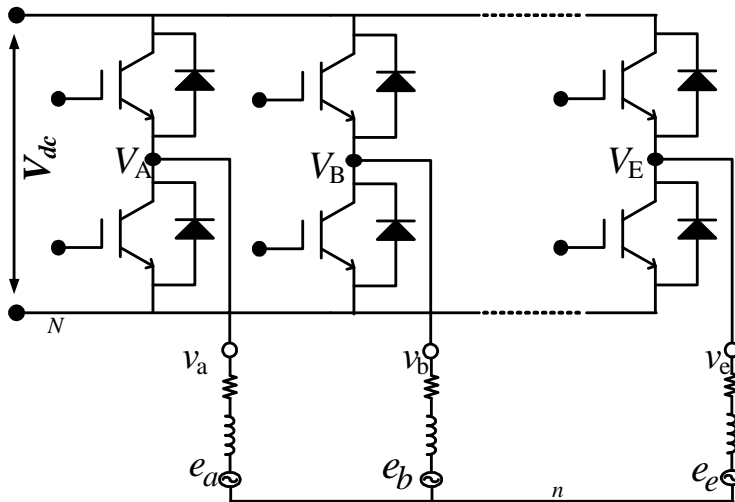


Figure 1. Five-phase voltage source inverter power circuit.

Phase-to-neutral voltages of the star connected load are most easily found by defining a voltage difference between the star point *n* of the load and the negative rail of the dc bus *N*. The following correlation then holds true:

$$\begin{aligned}
 v_A &= v_a + v_{nN} \\
 v_B &= v_b + v_{nN} \\
 v_C &= v_c + v_{nN} \\
 v_D &= v_d + v_{nN} \\
 v_E &= v_e + v_{nN}
 \end{aligned}
 \tag{1}$$

Since the phase voltages in a star connected load sum to zero, summation of the equations (1) yields

$$v_{nN} = (1/5)(v_A + v_B + v_C + v_D + v_E) \tag{2}$$

Substitution of (2) into (1) yields phase-to-neutral voltages of the load in the following form:

$$\begin{aligned} v_a &= (4/5)v_A - (1/5)(v_B + v_C + v_D + v_E) \\ v_b &= (4/5)v_B - (1/5)(v_A + v_C + v_D + v_E) \\ v_c &= (4/5)v_C - (1/5)(v_A + v_B + v_D + v_E) \\ v_d &= (4/5)v_D - (1/5)(v_A + v_B + v_C + v_E) \\ v_e &= (4/5)v_E - (1/5)(v_A + v_B + v_C + v_D) \end{aligned} \tag{3}$$

3. Five-phase drive structure

A simple open-loop five-phase drive structure is elaborated in Figure 2. The dc link voltage is adjusted from the controlled rectifier by varying the conduction angles of the thyristors. The frequency of the fundamental output is controlled from the IGBT based voltage source inverter. The inverter is operating in the quasi square wave mode instead of more complex PWM mode. Thus the overall control scheme is similar to a three-phase drive system. Since the inverter is operating in square wave mode the analogue circuit based controller is much simpler and cheaper compared to more sophisticated digital signal processor based control schemes. This type of solution is very cheap and convenient for use in coarse applications such as water pumping. These types of applications do not require fast dynamic response of drive systems and thus the need of high performance control schemes do not arise. The power quality of the remote locations in developing countries such as Indian subcontinents are not adequate for reliable and durable operation of sensitive microprocessors/microcontrollers/digital signal processors based controllers. It is thus intended to develop cheap and robust controller based on simple, and reliable analogue circuit components for such locations. The subsequent section describes the implantation issues of control of a five-phase voltage source inverter. The motivation behind choosing this structure lies in the fault tolerant nature of a five-phase drive system (Apsley et al., 2006).

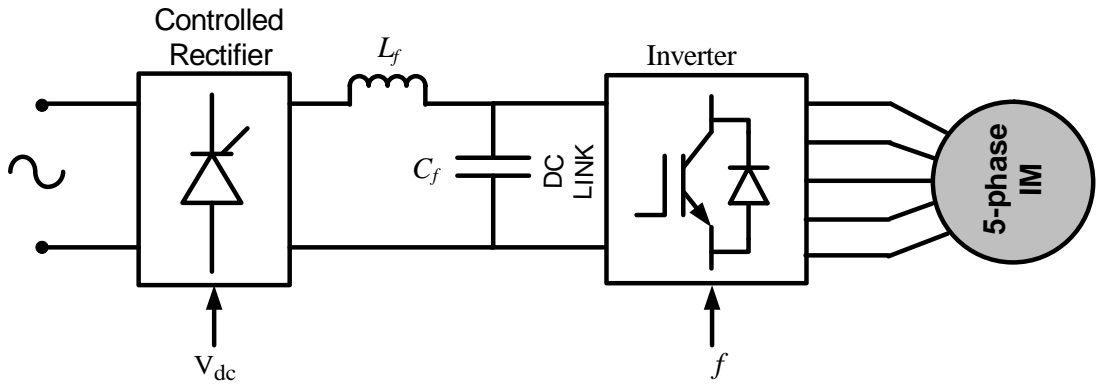


Figure 2. Five-phase induction Motor Drive structure.

4. Analogue circuit based five-phase voltage source inverter

To test the stepped operation in various conduction modes, a five-phase IGBT based prototype inverter is built in the laboratory, the block diagram of the control circuit of the Inverter is presented in Figure 3.

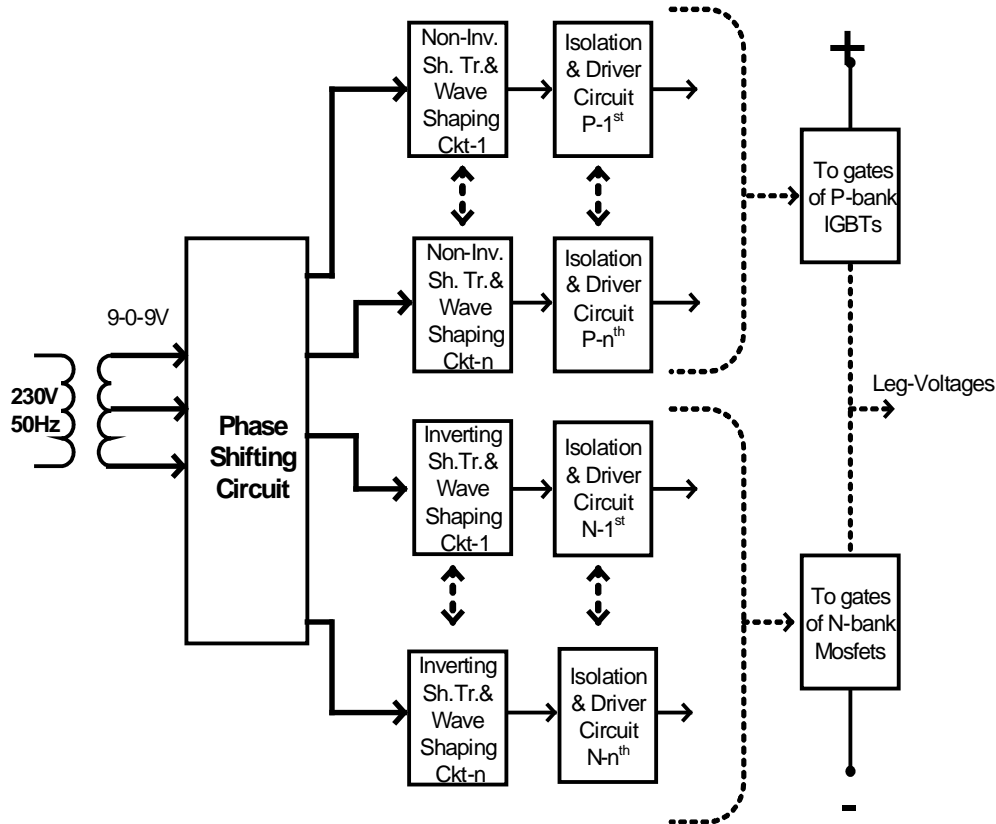


Figure 3. Block diagram of the complete control circuit.

Electric supply is taken from a single-phase grid and is converted to 9-0-9 V using a transformer, which is fed to the phase shifting circuit, to provide appropriate phase shift (i.e. 72° between each phase) for operation at various conduction angles. Here the phase shift is achieved at 50 Hz. However, for other than 50 Hz the required phase shift can be achieved using variable resistances in RC network of phase shifting circuit. The phase shifted signal is then fed to the inverting/non-inverting Schmitt trigger circuit and wave shaping circuit block which contains zero crossing detector. The processed signal is then fed to the isolation and driver circuit which is then finally given to the gate of IGBTs. There are two separate circuits for upper and lower legs of the inverter. NOT gates are not used to give complemented gate drives for lower leg devices, because complement of 144° is 216° i.e. lower devices shall be 'ON' for 216° .

5. Results and discussion

5.1. Five-phase VSI testing

Experiment is conducted for stepped operation of five-phase voltage source inverter with 180° (classical) and 144° (proposed) conduction modes for star connected five-phase resistive load at first. A single-phase supply is given to the control circuit through the phase shifting network. The output of the phase shifting circuit provides the required five-phase output voltage by appropriately tuning it as shown in Figure 4. These five-phase signals are then further processed to generate the pulses to the gate drive circuit. It is important to emphasise here that the poor power quality of the supply can be seen from the distorted waveforms of Figure 4. This is the power quality available in the laboratory setup, and thus the importance of the proposed solution can be understood at the remote locations.

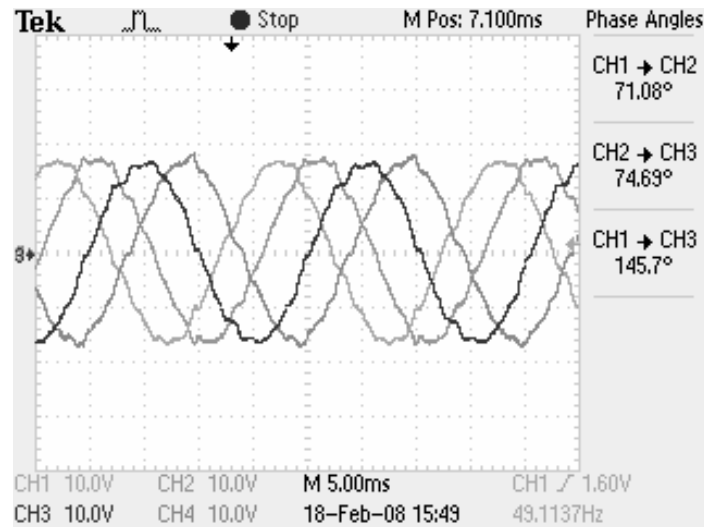


Figure 4. Five-phase output obtained from phase shifting network.

5. 1.1. 180° Conduction mode

Each switch is assumed to conduct for 180°, leading to the operation in the ten-step mode. Phase delay between firing of two switches in any subsequent two phases is equal to $360^\circ/5 = 72^\circ$. The corresponding phase voltages thus obtained are shown in Figure 5, keeping the dc link voltage at 60 V. The waveform is in ten step and is in full compliance with the finding of Ward and Harer (1969).

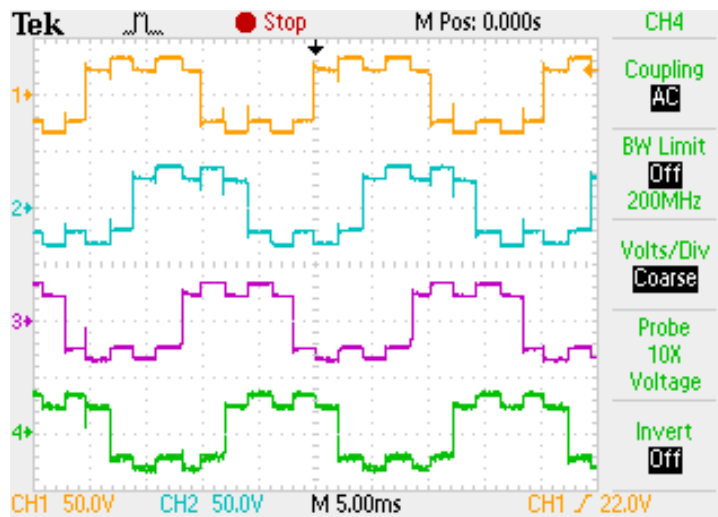


Figure 5. Output phase ‘a-d’ voltages for 180° conduction mode.

There are two systems of line voltages in a five-phase system namely adjacent and non-adjacent with phase shifts of 72° and 144°, respectively. Adjacent line voltages have lower magnitudes compared to the non-adjacent line voltages. Non-adjacent line voltage thus obtained is shown in Figure 6. All currents are measured using ac/dc current probe giving output of 100 mV/A.



Figure 6. Non-adjacent line voltage for 180° conduction mode with dc link voltage equal to 180 V.

5. 1.2. 144° conduction mode

The gate drive signal is such that each power switch remains on for 144° (or 80% duty cycle) and remains floating for 36° (or 20% duty cycle). This mode thus provides an inherent dead band in the switching of two power switches of the same leg. The output from the wave shaping circuit and the gate drive for two legs are shown in Figure 7 and Figure 8, respectively. The corresponding phase-to-neutral output voltage for phase ‘a’ is shown in Figure 9. Non-adjacent line voltage is presented in Figure 10.

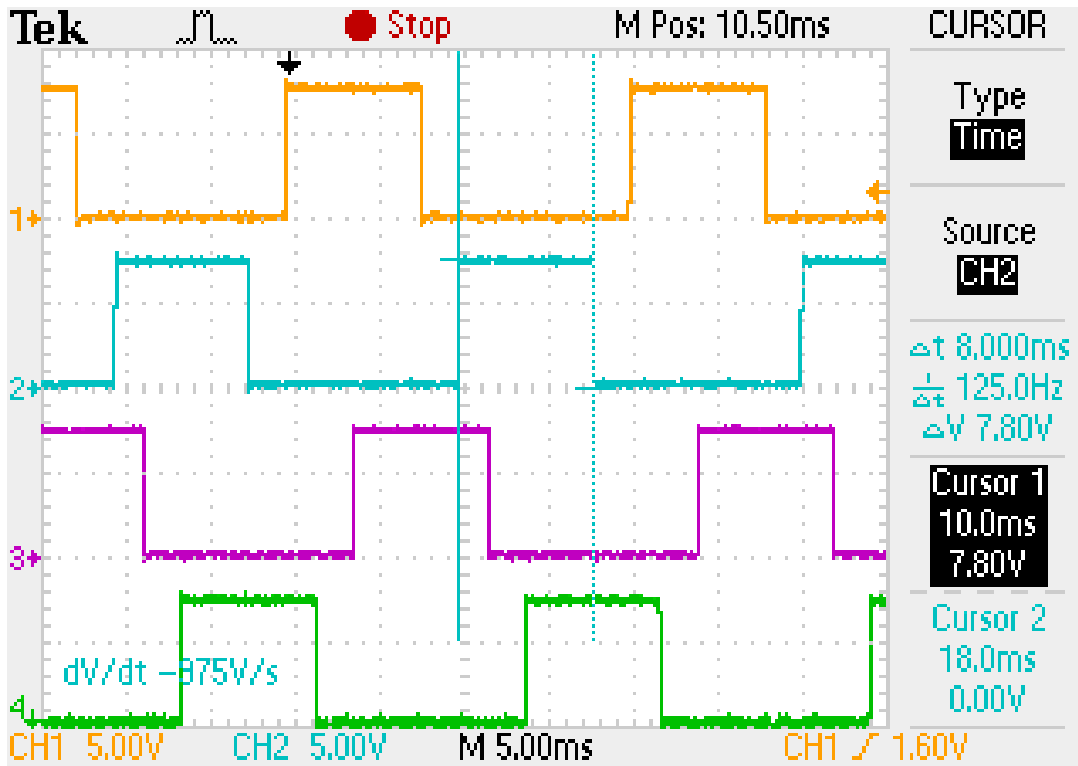


Figure 7. Output of wave shaping circuit for 144° conduction mode for leg A-B.

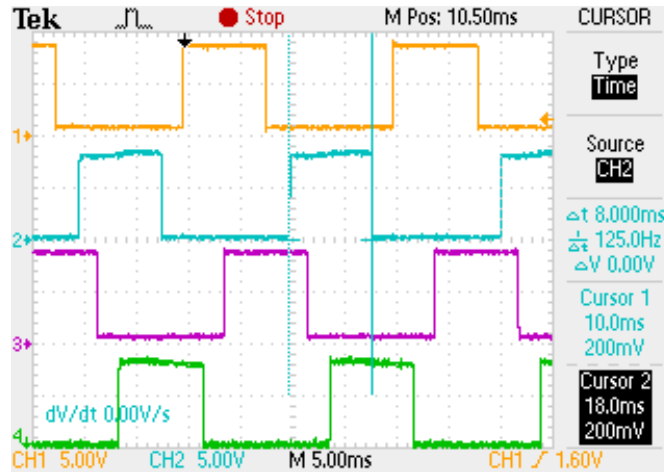


Figure 8. Gate Drive signals for leg A-B for 144° conduction mode.

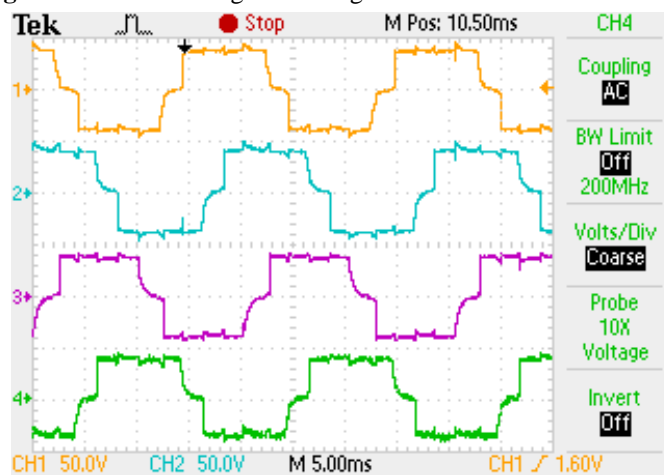


Figure 9. Output phase 'a-d' voltage for 144° conduction mode.



Figure 10. Non-adjacent line voltage for 144° conduction mode with dc link voltage equal to 180 V.

5. 2. Harmonic profile and torque pulsation reduction

5. 2.1. Inverter output waveform analysis

This section presents the comprehensive analysis of experimental results. The performance of two different conduction modes are elaborated in terms of the harmonic content in the phase voltages, line voltages and the distortion in the ac side line current.

The Fourier series of the phase-to-neutral voltage for 180° conduction mode is obtained as;

$$v(t) = \frac{2}{\pi} V_{DC} \left[\sin \omega t + \frac{1}{3} \sin 3\omega t + \frac{1}{7} \sin 7\omega t + \frac{1}{9} \sin 9\omega t + \frac{1}{11} \sin 11\omega t + \frac{1}{13} \sin 13\omega t + \dots \right] \tag{4}$$

From (4) it follows that the fundamental component of the output phase-to-neutral voltage has an RMS value equal to

$$V_1 = \frac{\sqrt{2}}{\pi} V_{dc} = 0.45V_{DC} . \tag{5}$$

The Fourier series of the phase-to-neutral voltage for 144° conduction mode is obtained as;

$$v(t) = \frac{2V_{dc}}{\pi} \sum_{n=1,2,3..}^{\infty} \left[\frac{\cos\left((2n-1)\frac{\pi}{10} \right) \sin((2n-1)\omega t)}{2n-1} \right] \tag{6}$$

From (6) it follows that the fundamental component of the output phase-to-neutral voltage has an RMS value equal to

$$V_1 = \frac{\sqrt{2}}{\pi} V_{dc} \cos\left(\frac{\pi}{10} \right) = 0.428V_{DC} \tag{7}$$

The loss in fundamental voltage in 144° conduction mode is of the order of 4.89% compared to 180° conduction mode. This loss will affect the loss of torque in the driven machine and subsequently the load will be affected. However, the drop in the torque is not very significant compared to the benefits obtained due to better harmonic performance. The harmonic analysis of, line voltage and input ac side line current is carried out for different conduction modes and the resulting waveforms are shown in Figures 11-14. The input side AC current of converter contains odd and even harmonics (Figure 14) for 144° conduction mode while a typical spectrum is depicted for 180° conduction mode.

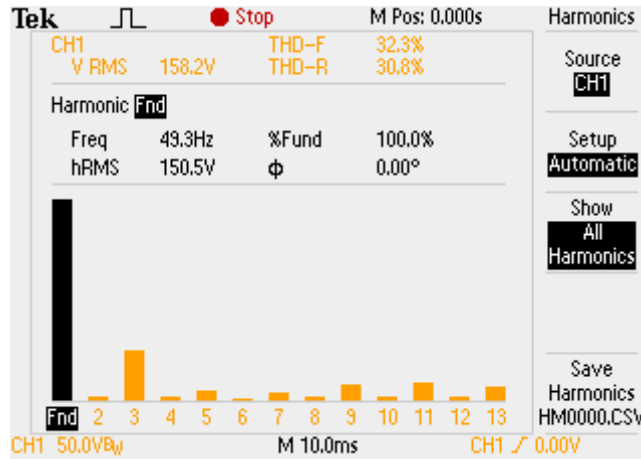


Figure 11. Spectrum of non-adjacent line voltage (Vac) for 180° conduction mode for dc link voltage of 180 V.

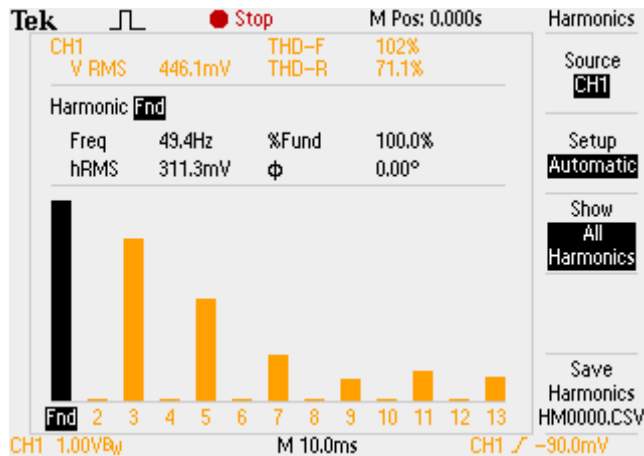


Figure 12. Spectrum of input side current for 180° conduction mode.

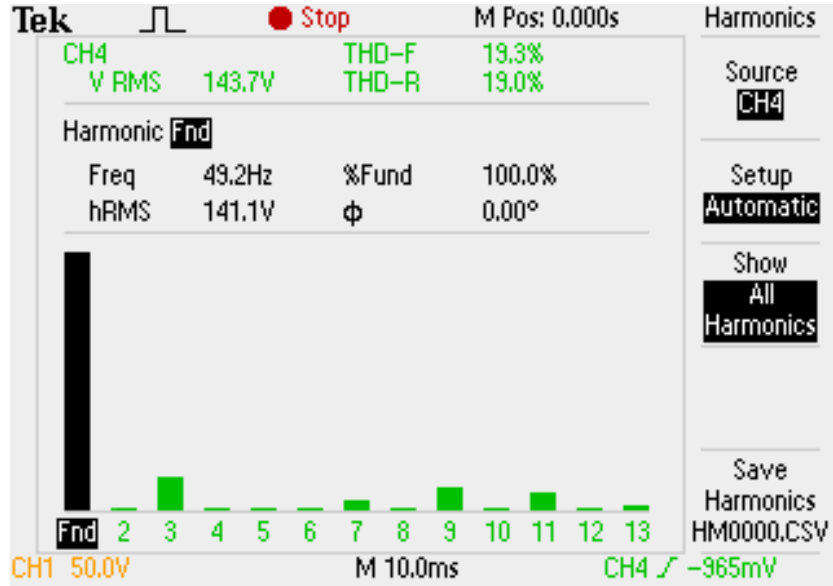


Figure 13. Spectrum of non-adjacent line 'Vac' voltage for 144° conduction mode for dc link voltage of 180 V.

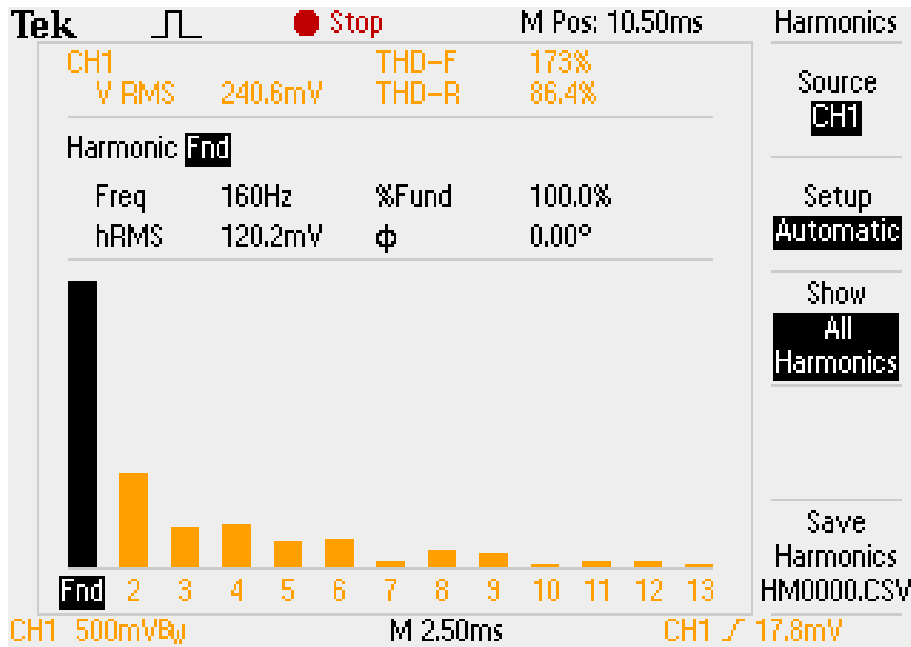


Figure 14. Spectrum of input side current for 144° conduction mode.

Performance comparison in terms of harmonic content in output phase voltage, output non-adjacent line voltage and input ac side current for different conduction modes are presented in Figures 15-17. It is clearly seen that the harmonic content reduces significantly with reduction in conduction angle. The harmonic content is largest in 180 degree conduction mode and it is least in 144 degree conduction mode. However, the best utilisation of available dc link voltage is possible with conventional ten step mode (180 degree conduction mode). It can thus be concluded that a trade-off exist between the loss in fundamental and corresponding gain in terms of lower harmonic content in output waveform is obtained by using 144 degree conduction mode.

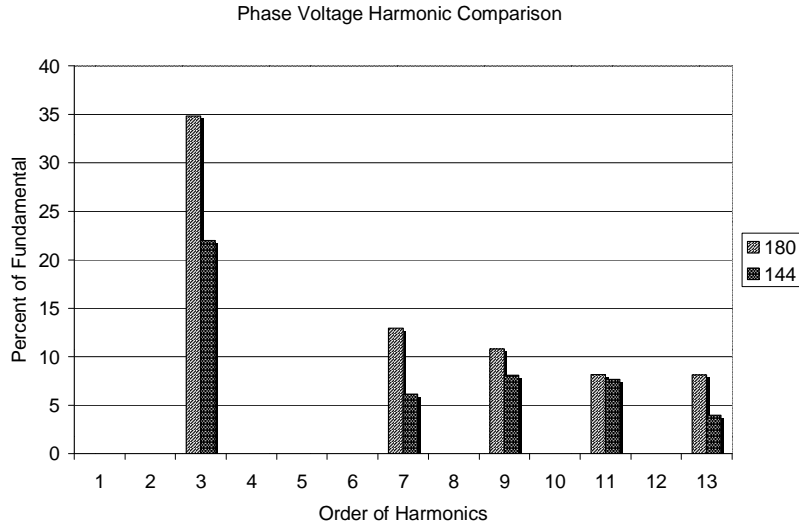


Figure 15. Harmonic content in output phase voltage for different conduction mode.

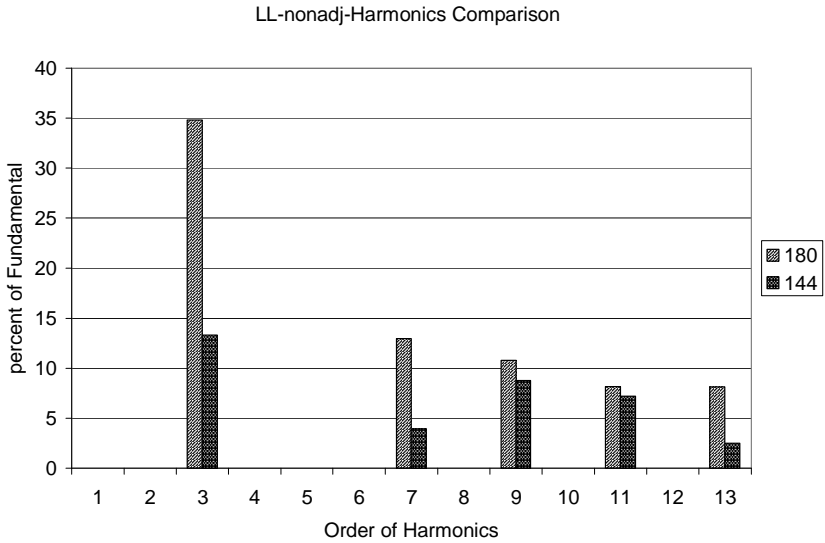


Figure 16. Harmonic content in output phase voltage for different conduction mode.

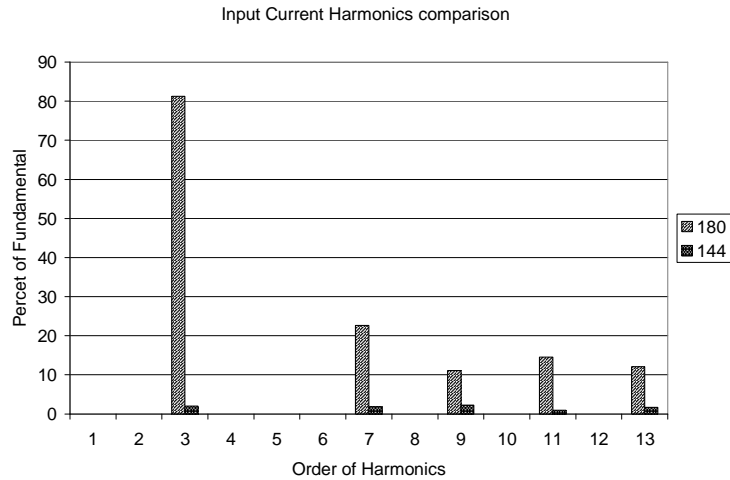


Figure 17. Harmonic content in input side ac current for different conduction mode.

A comparison of total harmonic distortion in the output phase voltages of five-phase voltage source inverter for different conduction angle is presented in Figure 18. The conduction angles considered are 180°, 162°, 144°, 126°, and 108°. Thus two more conduction states are included when compared to Figure 16 and Figure 17, to further prove the superiority of control at 144° conduction mode. It is observed from Figure 18 that the lowest THD is obtained for 144° conduction mode.

Comparison of Harmonics and THD

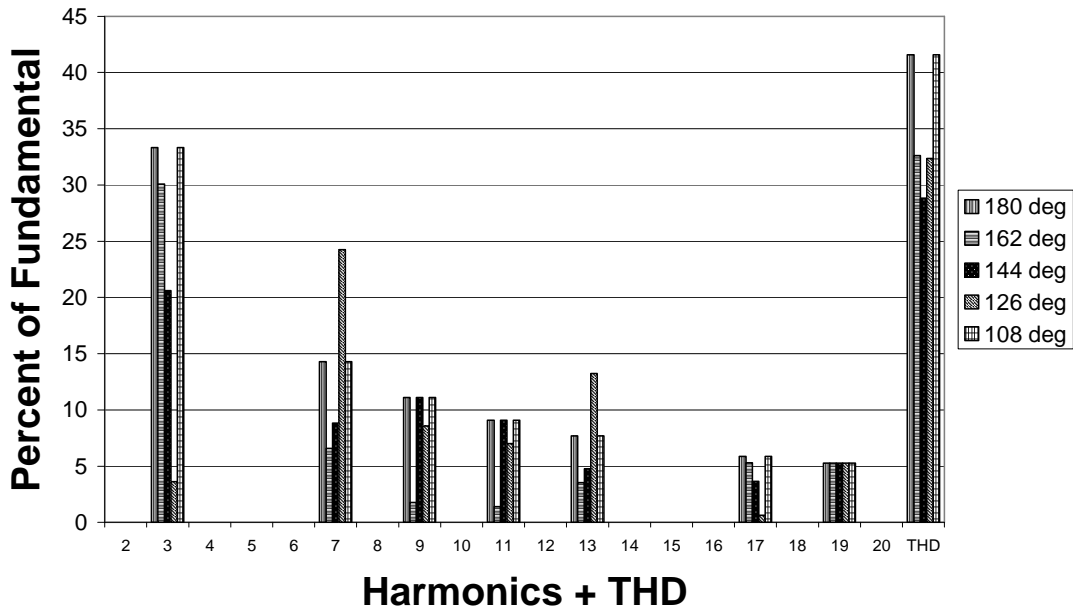


Figure 18. Comparison of Total Harmonic distortion at various conduction angles.

5. 2.2 Five-phase induction motor drive using the quasi square wave 5.2.2.1180 degree Conduction Mode

A Five-phase induction motor is supplied using the custom built five-phase inverter operating at 180° conduction mode and the dc link voltage is set to 200 V. The motor is allowed to run at one speed corresponding to 50 Hz output. The resulting non adjacent line voltage and the line current is depicted in Figure 19. It is observed from the waveform that current I_b leads the voltage V_{ac} by 54° (approximately), that means I_b is lagging V_b by 36° because phase difference between V_{ac} and V_b is 90°. The spectrum of the line voltage and current are shown in Figure 20 and Figure 21, respectively.

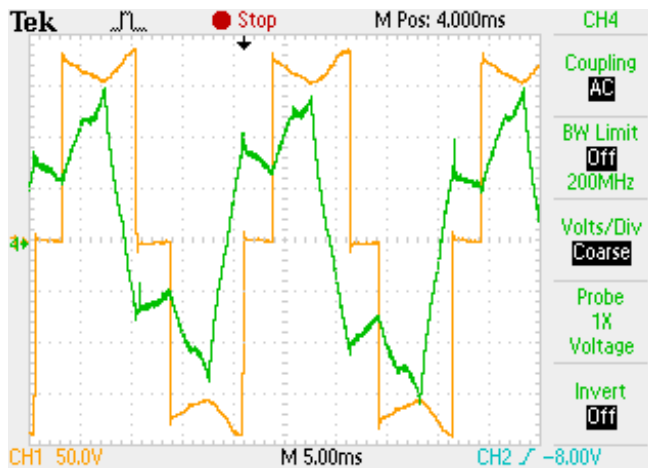


Figure 19. Non-adjacent line voltage V_{ac} and I_b (180° conduction mode).

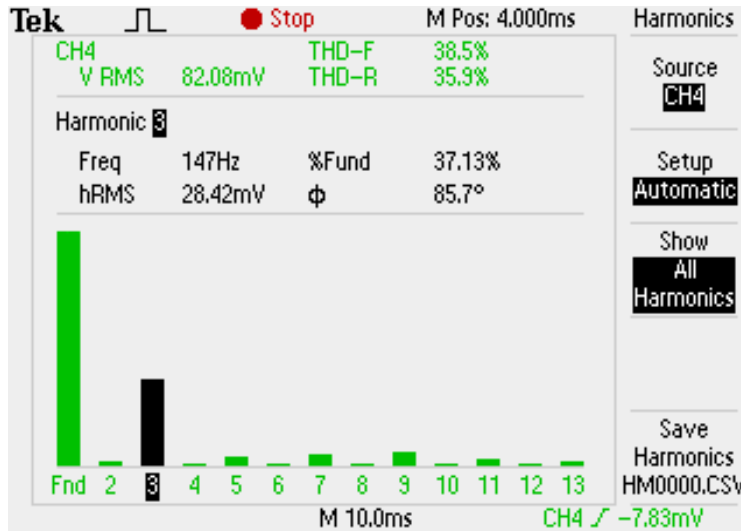


Figure 20. Line Current (I_b) harmonics (180° conduction mode)

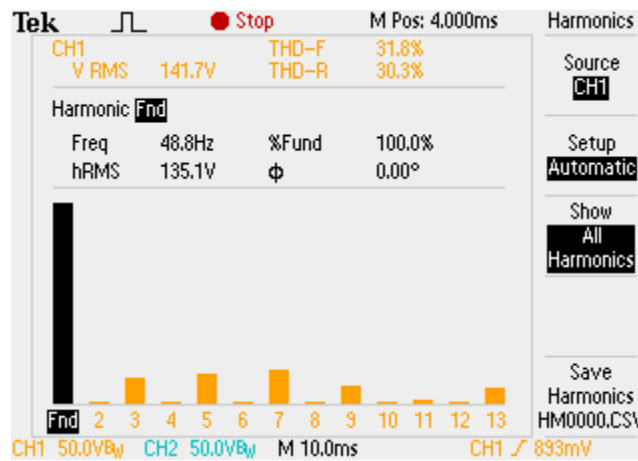


Figure 21. Non-adjacent Voltage (V_{ac}) Harmonics (180° conduction mode)

5.2.2.2144 degree Conduction Mode

The five-phase induction motor is further tested with the inverter operating at 144° conduction mode. The resulting line voltage and current waveforms are presented in Figure 22. The corresponding harmonic spectrum are shown in Figures 23 and 24.

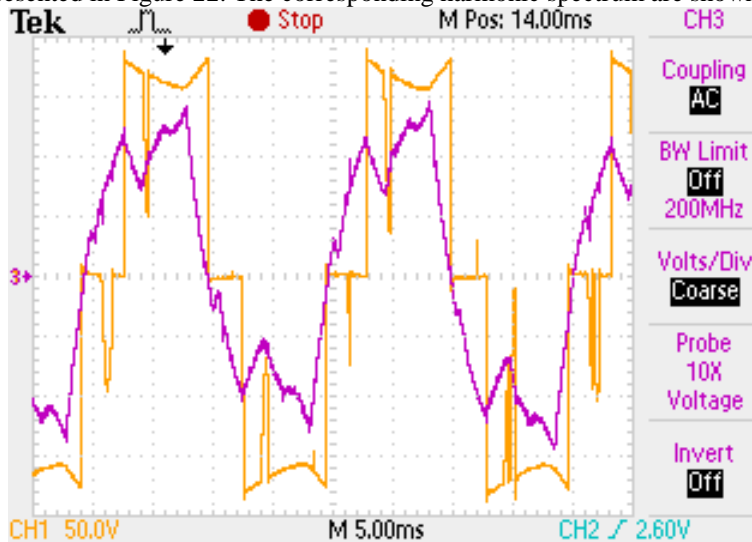


Figure 22. Non-adjacent L-L (V_{ac}) Voltage and Line Current (I_b) (144° conduction mode)

Here, current I_b leading the voltage V_{ac} by about 36° , that means I_b is lagging V_b by 54° . Here, even harmonics are negligible and 5^{th} harmonics is not zero. It is because of current flowing through the freewheeling diodes on inductive load. But harmonics are reduced in comparison to 180° conduction mode. These experimental results are in full agreement with that of simulated and analytical findings.

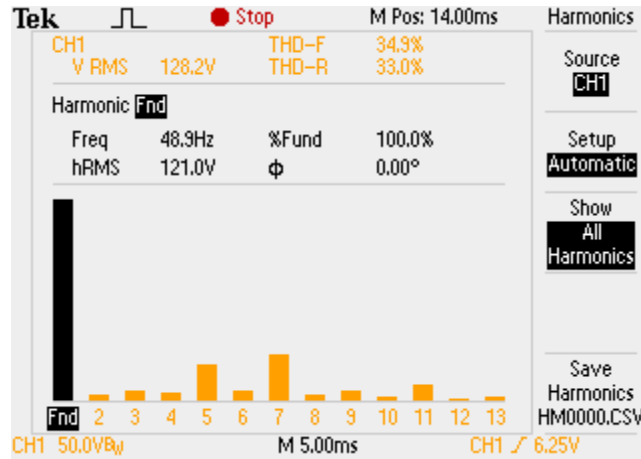


Figure 23. Harmonics Spectrum of Non-adjacent L-L (V_{ac}) Voltage (144° conduction mode)

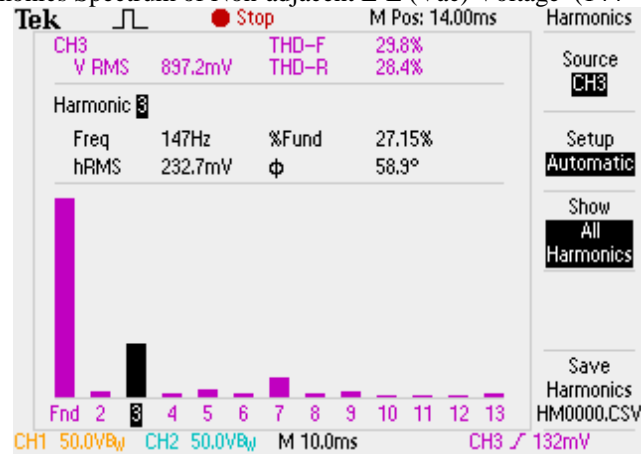


Figure 24. Harmonic Spectrum of Line Current I_b (144° conduction mode)

5. 2.3. Torque pulsation comparison

Pulsating torques are produced in an induction motor drive system when harmonic current interact with the fundamental air gap flux and also when the harmonic air gap flux interact with the fundamental rotor current, Bose (2002) and Krishnan (2001). The pulsating torques causes undesirable effects in the drive system by producing losses, vibration and noise. A quantitative assessment of torque pulsation in a three-phase drive and five-phase drive for stepped operation is done and presented in this section.

5.2.3.1 Three-phase drive

The predominant harmonics in a three-phase induction motor drive are 5^{th} and 7^{th} , with 5^{th} being backward rotating and 7^{th} being forward rotating both leading to 6^{th} harmonic pulsating torques, Bose (2002) and Krishnan (2001). The expression for the sixth harmonic pulsating torque is given as;

$$T_{e6} = \frac{3}{2}P[\Psi_{m1}(I_{r7} - I_{r5})\sin(6\omega_s t) + I_{r1}(\Psi_{m7} + \Psi_{m5})\cos(6\omega_s t)] \tag{8}$$

An expression is derived for the sixth harmonic pulsating torque in terms of fundamental voltage and equivalent circuit parameter and is obtained as;

$$(T_{e6})_{180^\circ} = K\left(\frac{3}{2}\right)\left[\left[\frac{\sin(7\omega_s t)}{49} - \frac{\sin(5\omega_s t)}{25}\right]\sin(6\omega_s t) + \left(\frac{1}{2}\right)\left[\frac{\sin(7\omega_s t)}{49} + \frac{\sin(5\omega_s t)}{25}\right]\cos(6\omega_s t)\right] \tag{9}$$

Where $K = \left(\frac{PV_1}{\omega_s X_{eq}}\right)\left(\frac{2V_{DC}}{\pi}\right)$, and Ψ_{mk} is the peak of k^{th} harmonic mutual flux, V_1 is the fundamental applied voltage, X_{eq}

is the equivalent leakage reactance and P is the number of poles of induction machine

5.2.3.2 Five-phase drive

The predominant harmonics in a five-phase machine are 9th and 11th, with 9th being backward rotating and 11th being forward rotating both leading to 10th harmonic torques, Iqbal et al. (2008). The detailed derivation of the torque pulsation is presented in Appendix 1.

The tenth harmonic pulsating torque for 180° conduction mode is obtained as;

$$(T_{e10})_{180^\circ} = \frac{5}{2} P [\psi_{m1}(I_{r11} - I_{r9}) \sin(10\omega t) + I_{r1}(\psi_{m11} + \psi_{m9}) \cos(10\omega t)] \tag{10}$$

The tenth harmonic pulsating torque for 144° conduction mode is obtained as;

$$(T_{e10})_{144^\circ} = \frac{5}{2} P [\psi_{m1}(I_{r11} - I_{r9}) \sin(10\omega t) + I_{r1}(\psi_{m11} + \psi_{m9}) \cos(10\omega t)] \tag{11}$$

An expression is derived for the tenth harmonic pulsating torque in terms of fundamental voltage and equivalent circuit parameter and is obtained as;

$$(T_{e10})_{180^\circ} = \frac{5}{2} \left(\frac{PZ}{\omega_s X_{eq}} \right) \left(\frac{2V_{Dc}}{\pi} \right)^2 \sin(\alpha) [\sin(10\omega t + \alpha)]$$

$$(T_{e10})_{144^\circ} = \frac{-5}{2} \left(\frac{PZ}{\omega_s X_{eq}} \right) \left(\frac{2V_{Dc}}{\pi} \right)^2 \cos^2\left(\frac{\pi}{10}\right) \sin(\alpha) [\sin(10\omega t + \alpha)] \tag{12}$$

Where;

$$Z = \sqrt{A^2 + B^2}, A = Z \cos(\alpha), B = Z \sin(\alpha), \alpha = \tan^{-1} \frac{B}{A},$$

$$A = \left(\frac{1}{(11)^2} \sin(11\omega_s t) - \frac{1}{(9)^2} \sin(9\omega_s t) \right)$$

$$B = \frac{1}{2} \left(\frac{1}{(11)^2} \sin(11\omega_s t) + \frac{1}{(9)^2} \sin(9\omega_s t) \right)$$

Thus the ratio of pulsating torques for a typical motor in two conduction modes is obtained as;

$$\frac{|(T_{e10})_{144^\circ}|}{|(T_{e10})_{180^\circ}|} = \cos^2\left(\frac{\pi}{10}\right) = 0.9045084972 \tag{13}$$

$$\frac{(Te_6)_{180^\circ}}{(Te_{10})_{180^\circ}} = \frac{1.4 \times 10^{-15}}{2 \times 10^{-16}} = 7.0 \tag{14}$$

$$\frac{(Te_6)_{180^\circ}}{(Te_{10})_{144^\circ}} = \frac{1.4 \times 10^{-15}}{1.8 \times 10^{-16}} = 7.78 \tag{15}$$

The relations (13-15) show, there is reduction in torque ripples in five phase motor at 144° conduction mode by 10% (approx) when compared with 180° conduction mode of five phase motor, 700% when compared with 180° conduction modes of five phase motors, and 778% when compared with 180° conduction mode of three phase motor and 144° conduction mode of five phase motor.

6. Conclusion

The paper presents a solution of electric drive system supplied from weak grid with poor power quality. The proposed solution lies in the use of inverter fed five-phase induction motor drive system with stepped operation of the inverter. The inverter is proposed to operate in newly proposed 144° conduction mode. This offers better harmonic performance and thus lower losses, higher efficiency and better running cost. A comparison in torque pulsation is also presented which suggest significant reduction in torque pulsation by adopting the proposed 144° conduction mode. Analytical and experimental approach is used to validate the findings.

Nomenclature

- T_{e10} Tenth Harmonic torque
- T_{e6} Sixth Harmonic torque
- V_1 Fundamental Voltage
- V_{dc} DC Link Voltage
- v_{nN} Common mode voltage

v_a	Phase voltage
v_A	Leg Voltage
Ψ	Flux Linkage

Appendix I: Torque Pulsation for 180° conduction mode in a five-phase induction motor drive

$$\begin{aligned} (T_{e10})_{180^\circ} &= \frac{5}{2} P [\psi_{m1} (I_{r11} - I_{r9}) \sin(10\omega_s t) + I_{r1} (\psi_{m11} + \psi_{m9}) \cos(10\omega_s t)] \\ &= \frac{5}{2} P \left[\frac{V_1}{\omega_s} \left(\frac{V_{11}}{11X_{eq}} - \frac{V_9}{9X_{eq}} \right) \sin(10\omega_s t) + \frac{V_1}{2X_{eq}} \left(\frac{V_{11}}{11\omega_s} - \frac{V_9}{9\omega_s} \right) \cos(10\omega_s t) \right] \end{aligned} \quad (\text{AI.1})$$

The above equation is the defining equation of the tenth harmonic pulsating torque as given in equation (9). After substituting the equations for V_{11} (magnitude of the eleventh harmonic voltage component), the following equation results;

$$= \frac{5}{2} \left(\frac{P_1}{\omega_s X_{eq}} \right) \left(\frac{2V_{DC}}{\pi} \right) \sin(\omega_s t) \left[\left(\frac{2V_{DC}}{(11)^2 \pi} \sin(11\omega_s t) - \frac{2V_{DC}}{(9)^2 \pi} \sin(9\omega_s t) \right) \sin(10\omega_s t) + \frac{1}{2} \left(\frac{2V_{DC}}{(11)^2 \pi} \sin(11\omega_s t) + \frac{2V_{DC}}{(9)^2 \pi} \sin(9\omega_s t) \right) \cos(10\omega_s t) \right] \quad (\text{AI.2})$$

Where the fluxes and currents are further given as;

$$\psi_{m1} = \frac{V_1}{2\omega_s}, \psi_{m9} = \frac{V_9}{2 \times 9\omega_s}, \psi_{m11} = \frac{V_{11}}{2 \times 11\omega_s}, I_{r1} = \frac{V_1}{X_{eq}}, I_{r9} = \frac{V_9}{9X_{eq}}, I_{r11} = \frac{V_{11}}{11X_{eq}}, \quad (\text{AI.3})$$

After substituting the flux and current relations from A3 to A2, the equation can be written as;

$$= \frac{5}{2} \left(\frac{P}{\omega_s X_{eq}} \right) \left(\frac{2V_{DC}}{\pi} \right)^2 \sin(\omega_s t) \left[\left(\frac{1}{(11)^2} \sin(11\omega_s t) - \frac{1}{(9)^2} \sin(9\omega_s t) \right) \sin(10\omega_s t) + \frac{1}{2} \left(\frac{1}{(11)^2} \sin(11\omega_s t) + \frac{1}{(9)^2} \sin(9\omega_s t) \right) \cos(10\omega_s t) \right] \quad (\text{AI.4})$$

$$\text{where } V_1 = \frac{2V_{DC}}{\pi} \sin(\omega_s t), V_9 = \frac{2V_{DC}}{9\pi} \sin(9\omega_s t), V_{11} = \frac{2V_{DC}}{11\pi} \sin(11\omega_s t) \quad (\text{AI.5})$$

$$\begin{aligned} \text{where } A &= \left(\frac{1}{(11)^2} \sin(11\omega_s t) - \frac{1}{(9)^2} \sin(9\omega_s t) \right), B = \frac{1}{2} \left(\frac{1}{(11)^2} \sin(11\omega_s t) + \frac{1}{(9)^2} \sin(9\omega_s t) \right) \\ &= \frac{5}{2} \left(\frac{P}{\omega_s X_{eq}} \right) \left(\frac{2V_{DC}}{\pi} \right)^2 \sin(\omega_s t) \left[(Z \cos(\alpha)) \sin(10\omega_s t) + (Z \sin(\alpha)) \cos(10\omega_s t) \right] \end{aligned} \quad (\text{AI.6})$$

$$\text{where } A = Z \cos(\alpha), B = Z \sin(\alpha), Z = \sqrt{A^2 + B^2}, \alpha = \tan^{-1} \frac{B}{A}$$

Finally the equation for the tenth harmonic pulsating torque is obtained as;

$$(T_{e10})_{180^\circ} = \frac{5}{2} \left(\frac{PZ}{\omega_s X_{eq}} \right) \left(\frac{2V_{DC}}{\pi} \right)^2 \sin(\omega_s t) \left[\sin(10\omega_s t + \alpha) \right] \quad (\text{AI.7})$$

Similarly the tenth harmonic torque pulsation for 144° conduction mode in a five-phase induction motor drive is derives as;

$$(T_{e10})_{144^\circ} = \frac{5}{2} P [\psi_{m1} (I_{r11} - I_{r9}) \sin(10\omega_s t) + I_{r1} (\psi_{m11} + \psi_{m9}) \cos(10\omega_s t)] \quad (\text{AI.8})$$

The above equation is the defining equation for the pulsating torque. After substituting the fluxes the following equation results;

$$\begin{aligned}
 &= \frac{5}{2} P \left[\frac{V_1}{\omega_s} \left(\frac{V_{11}}{11X_{eq}} - \frac{V_9}{9X_{eq}} \right) \text{Sin}(10\omega_s t) + \frac{V_1}{2X_{eq}} \left(\frac{V_{11}}{11\omega_s} - \frac{V_9}{9\omega_s} \right) \text{Cos}(10\omega_s t) \right] \\
 &= \frac{5}{2} \left(\frac{P_1}{\omega_s X_{eq}} \right) \left(\frac{2V_{DC}}{\pi} \right) \text{Cos} \left(\frac{\pi}{10} \right) \text{Sin}(\omega_s t) \left[\left(\frac{2V_{DC}}{(11)^2 \pi} \text{Cos} \left(\frac{11\pi}{10} \right) \text{Sin}(11\omega_s t) - \frac{2V_{DC}}{(9)^2 \pi} \text{Cos} \left(\frac{9\pi}{10} \right) \text{Sin}(9\omega_s t) \right) \text{Sin}(10\omega_s t) \right. \\
 &\quad \left. + \frac{1}{2} \left(\frac{2V_{DC}}{(11)^2 \pi} \text{Cos} \left(\frac{11\pi}{10} \right) \text{Sin}(11\omega_s t) + \frac{2V_{DC}}{(9)^2 \pi} \text{Cos} \left(\frac{9\pi}{10} \right) \text{Sin}(9\omega_s t) \right) \text{Cos}(10\omega_s t) \right] \quad \text{(AI.9)}
 \end{aligned}$$

where $V_1 = \frac{2V_{DC}}{\pi} \text{Cos} \left(\frac{\pi}{10} \right) \text{Sin}(\omega_s t)$, $V_9 = \frac{2V_{DC}}{9\pi} \text{Cos} \left(\frac{9\pi}{10} \right) \text{Sin}(9\omega_s t)$, $V_{11} = \frac{2V_{DC}}{11\pi} \text{Cos} \left(\frac{11\pi}{10} \right) \text{Sin}(11\omega_s t)$ (AI.10)

$$\Psi_{m1} = \frac{V_1}{2\omega_s}, \Psi_{m9} = \frac{V_9}{2 \times 9\omega_s}, \Psi_{m11} = \frac{V_{11}}{2 \times 11\omega_s}, I_{r1} = \frac{V_1}{X_{eq}}, I_{r9} = \frac{V_9}{9X_{eq}}, I_{r11} = \frac{V_{11}}{11X_{eq}}, \quad \text{(AI.11)}$$

Substituting equations A10 and A11 into equation A9 yield;

$$\begin{aligned}
 &= \frac{5}{2} \left(\frac{P}{\omega_s X_{eq}} \right) \left(\left(\frac{2V_{DC}}{\pi} \right)^2 \text{Cos} \left(\frac{\pi}{10} \right) \text{Cos} \left(\frac{9\pi}{10} \right) \text{Sin}(\omega_s t) \right) \left[\left(\frac{1}{(11)^2} \text{Sin}(11\omega_s t) - \frac{1}{(9)^2} \text{Sin}(9\omega_s t) \right) \text{Sin}(10\omega_s t) \right. \\
 &\quad \left. + \frac{1}{2} \left(\frac{1}{(11)^2} \text{Sin}(11\omega_s t) + \frac{1}{(9)^2} \text{Sin}(9\omega_s t) \right) \text{Cos}(10\omega_s t) \right] \quad \text{(AI.12)}
 \end{aligned}$$

Since $\text{Cos} \left(\frac{9\pi}{10} \right) = \text{Cos} \left(\frac{11\pi}{10} \right)$

$$\begin{aligned}
 &= \frac{5}{2} \left(\frac{P}{\omega_s X_{eq}} \right) \left(\left(\frac{2V_{DC}}{\pi} \right)^2 \text{Cos} \left(\frac{\pi}{10} \right) \text{Cos} \left(\frac{9\pi}{10} \right) \text{Sin}(\omega_s t) \right) \left[(A) \text{Sin}(10\omega_s t) + (B) \text{Cos}(10\omega_s t) \right] \quad \text{(AI.13)}
 \end{aligned}$$

where $A = \left(\frac{1}{(11)^2} \text{Sin}(11\omega_s t) - \frac{1}{(9)^2} \text{Sin}(9\omega_s t) \right)$, $B = \frac{1}{2} \left(\frac{1}{(11)^2} \text{Sin}(11\omega_s t) + \frac{1}{(9)^2} \text{Sin}(9\omega_s t) \right)$

$$\begin{aligned}
 &= -\frac{5}{2} \left(\frac{P}{\omega_s X_{eq}} \right) \left(\left(\frac{2V_{DC}}{\pi} \right)^2 \text{Cos}^2 \left(\frac{\pi}{10} \right) \text{Sin}(\omega_s t) \right) \left[(Z \text{Cos}(\alpha)) \text{Sin}(10\omega_s t) + (Z \text{Sin}(\alpha)) \text{Cos}(10\omega_s t) \right]
 \end{aligned}$$

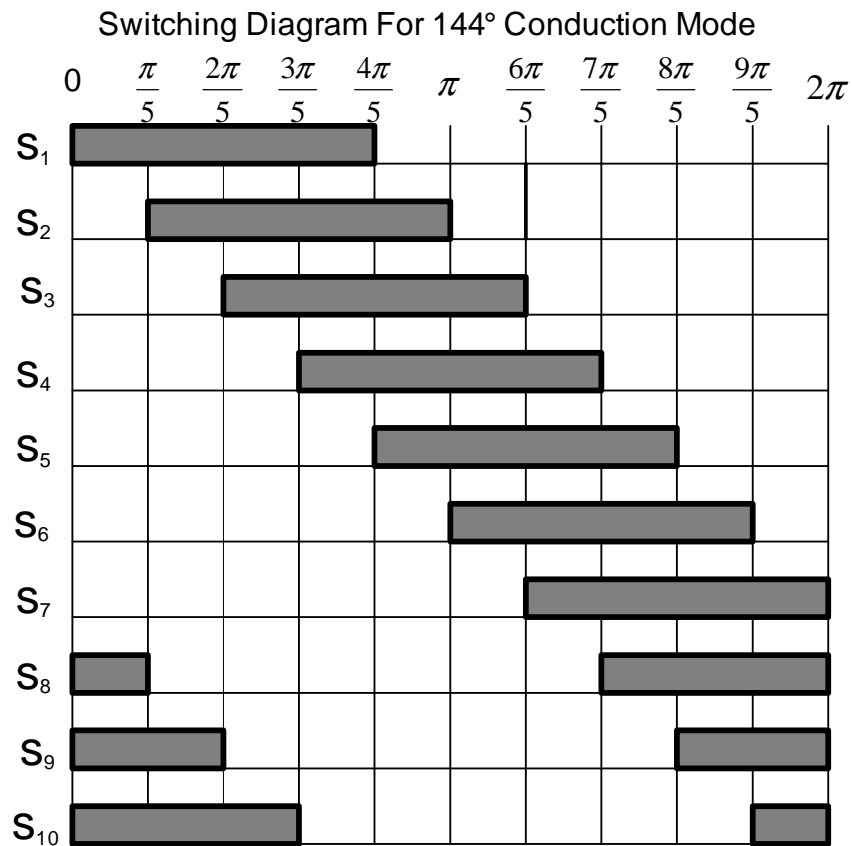
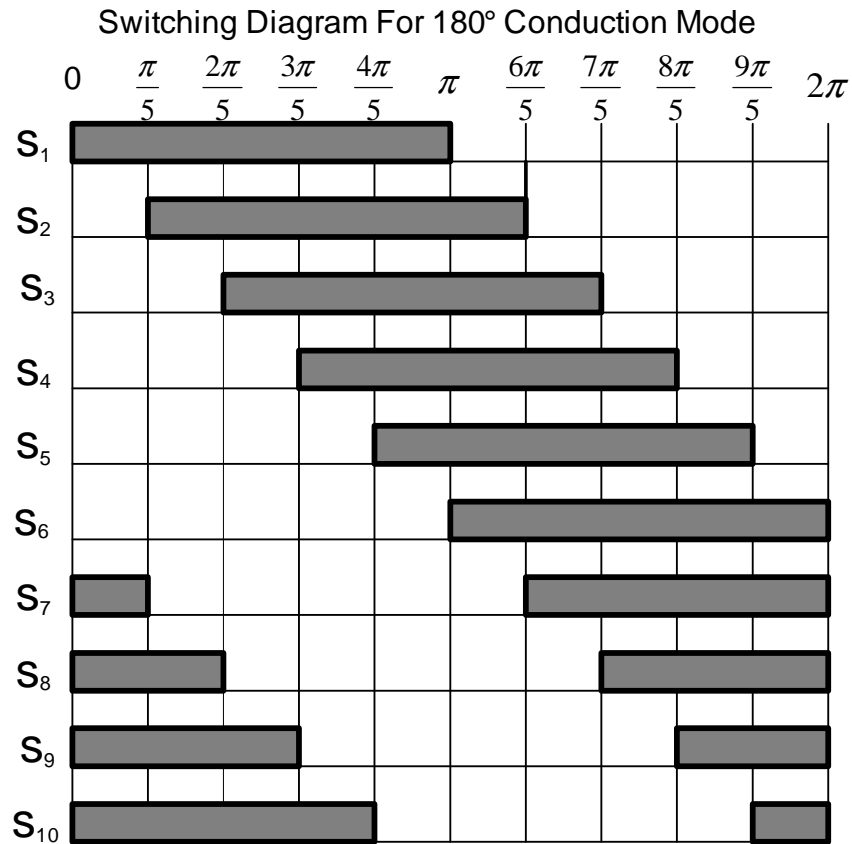
where $A = Z \text{Cos}(\alpha)$, $B = Z \text{Sin}(\alpha)$, $Z = \sqrt{A^2 + B^2}$, $\alpha = \text{Tan}^{-1} \frac{B}{A}$, $\text{Cos} \left(\frac{9\pi}{10} \right) = -\text{Cos} \left(\frac{\pi}{10} \right)$ (AI.14)

Finally the torque equation for tenth harmonic pulsation for 144° conduction is obtained as

$$(T_{e10})_{144^\circ} = -\frac{5}{2} \left(\frac{PZ}{\omega_s X_{eq}} \right) \left(\left(\frac{2V_{DC}}{\pi} \right)^2 \text{Cos}^2 \left(\frac{\pi}{10} \right) \text{Sin}(\omega_s t) \right) \left[\text{Sin}(10\omega_s t + \alpha) \right] \quad \text{(AI.15)}$$

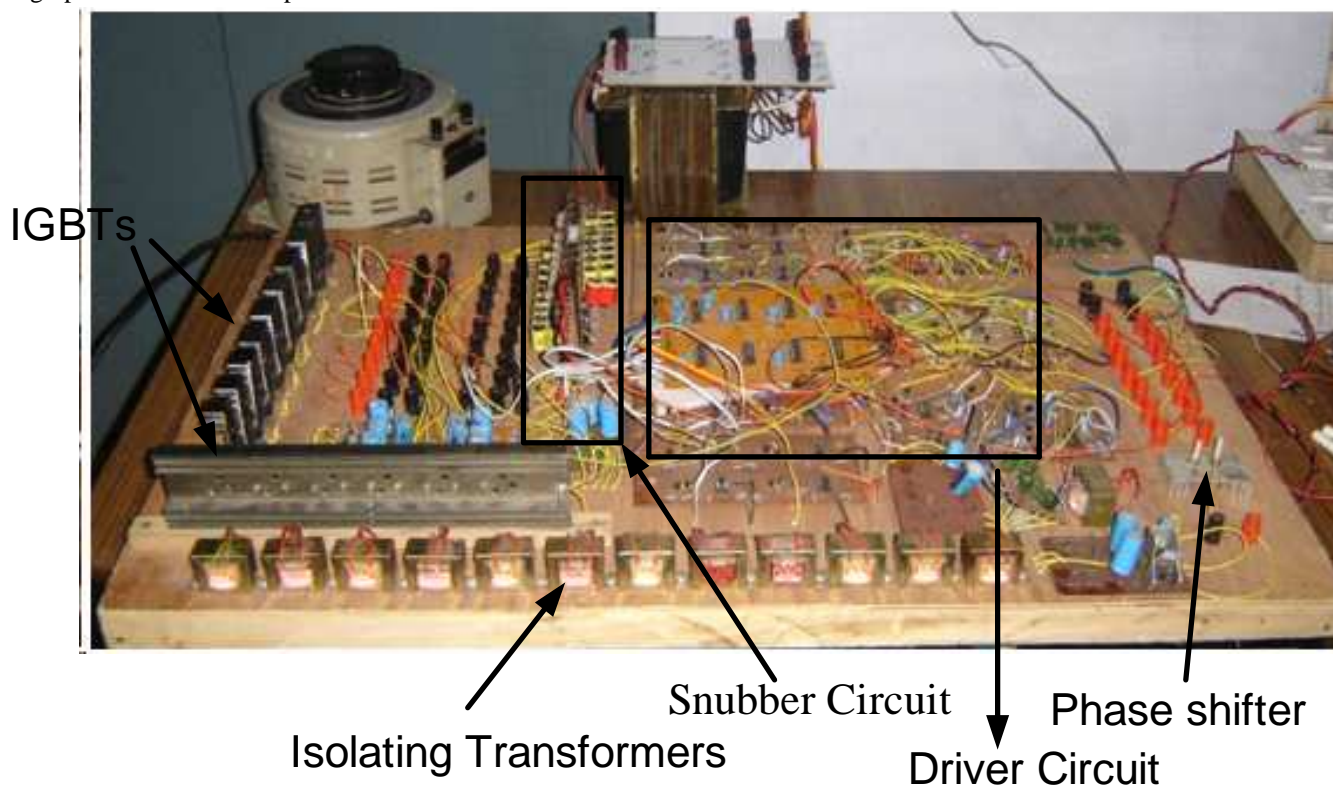
Appendix II:

Switching diagram for the two conduction mode:



Appendix III

Photograph of the entire set-up:



Appendix IV:

Table of components and their cost (For Driver Circuit Only)

Name of components	Specifications	Quantity	Cost (in Indian Rupees)
Step down Transformer	230 V to 12-0-12, 100mA	8	240/-
Operational Amplifier	uA-741	10	50/-
Voltage Regulator IC	7812	7	50/-
Opto-couplers	4N35	10	50/-
Presets	47K	10	20/-
Resistances	1K, 10K, etc (1/4 W)	100	20/-
Capacitors	0.1 microF, 1000 microF, etc	20	100/-
Printed Circuit Boards	general	6	60/-
Hardware	Screws, nuts & bolts, etc	-	20/-
Wooden board	-	-	30/-
Terminals	5 amp	20	100/-
Total Cost (in Indian Rupees)			740/-
Total Cost (in US\$)			16.44

Acknowledgements

Authors gratefully acknowledge the support provided by CSIR, New Delhi, India project no. 22(0420)/EMR-II/07 for the work.

References

- Apsley, J.M., Williamson, S., Smith, A.C., and Barnes, M., 2006. Induction motor performance as a function of phase number, *IEE Proc. Electric Power Applications*, Vol. 153, No. 6, pp. 898-904, 2006.
- Arahal, M.R. and Duran, M.J., 2009. PI tuning of Five-phase drives with third harmonic injection, *Control Engg. Practice*, Vol. 17, pp. 787-797, Feb.

- Bojoi, R., Farina, F., Profumo, F., and Tenconi, 2006. Dual three induction machine drives control - A survey, *IEEE Tran. On Ind. Appl.*, Vol. 126, No. 4, pp. 420-429.
- Bose, B.K., 2002. *Power Electronics and AC Drives*, Prentice Hall, New Jersey.
- Duran, M.J., Salas, F., Arahal, M.R., 2008. Bifurcation analysis of five-phase induction motor drives with third harmonic injection, *IEEE Trans. on Ind. Elect.* Vol. 55, No. 5, pp. 2006-2014, May.
- Golubev, A.N., and Ignatenko, S.V., 2000. Influence of number of stator-winding phases on the noise characteristics of an asynchronous motor, *Russian Electrical Engineering*, Vol. 71, No. 6, pp. 41-46, 2000.
- Hodge, C., Williamson, S., and Smith, S., 2002. Direct drive propulsion motors, *Proc. Int. Conf. on Electrical Machines ICEM*, Bruges, Belgium, Paper no. 087.
- Iqbal, A., and Levi, E., 2005. Space vector modulation scheme for a five-phase voltage source inverter, *Proc. European Power Electronics and Appl. Conf., EPE*, Dresden, Germany, CD-ROM paper 0006.
- Iqbal, A., Moinuddin, S., and Moin, A, Sk. 2008. Quantitative assessment of torque pulsation in inverter fed five-phase induction motor drive system”, *Proceedings of IEEE Region 10 Conference (TENCON 2008)*, University of Hyderabad, Hyderabad, Andhra Pradesh, India. Paper No. 1569126802.
- Jones, M., and Levi, E., 2002. A literature survey of state-of-the-art in multiphase ac drives, *Proc. 37th Int. Universities Power Eng. Conf. UPEC*, Stafford, UK, pp. 505-510.
- Krishnan, R., 2001. *Electric Motor Drives-Modelling, Analysis, and Control*, Prentice Hall, New Jersey.
- Levi, E., Bojoi, R., Profumo, F., Toliyat, H.A and Williamson, S., 2007. Multi-phase induction motor drives-A technology status review, *IET Elect. Power Appl.* Vol. 1, No. 4, pp. 489-516.
- Levi, E., 2008a. Guest editorial, *IEEE Trans. Ind. Electronics*, Vol. 55, No. 5, May, pp. 1891-1892.
- Levi, E., 2008b. Multi-phase machines for variable speed applications, *IEEE Trans. Ind. Elect.*, Vol. 55, No. 5, May, pp. 1893-1909.
- Lyra, R.,O., C., and Lipo, T., A. 2002. Torque density improvement in a six-phase induction motor with third harmonic current injection”, *IEEE Trans. Ind. Appl.*, Vol. 38, No. 5, pp. 1351-1360, Sept./Oct.
- Singh, G.K., 2002. Multi-phase induction machine drive research – a survey, *Electric Power System Research*, Vol. 61, pp. 139-147.
- Shi, R., Toliyat, H.A., and El-Antably, A., 2001. Field oriented control of five-phase synchronous reluctance motor drive with flexible 3rd harmonic current injection for high specific torque, *Conf. Rec. IEEE IAS Annual Meeting*, Chicago, IL, pp. 2097-2103.
- Ward, E.E., and H'arer, H., 1969. Preliminary investigation of an inverter-fed 5-phase induction motor, *Proc. IEE* Vol. 116, No. 6, pp. 980-984.
- Xu, H., Toliyat, H.A, and Petersen, L. J., 2001a, Five-phase induction motor drives with DSP-based control system,” *Proc. IEEE Int. Elec. Mach. And Drives Conf. IEMDC2001*, Cambridge, MA, pp. 304-309.
- Xu, H., Toliyat, H.A, and Petersen, L. J., 2001b. Rotor field oriented control of a five-phase induction motor with the combined fundamental and third harmonic injection, *Proc. IEEE Applied Power Elec. Conf. APEC*, Anaheim, CA, pp. 608-614, 2001.
- Williamson, S., and Smith, S., 2003. Pulsating torque and losses in multiphase induction machines, *IEEE Trans. On Ind. Appl.* Vol. 39, No. 4, pp. 986-993.

Biographical notes

Shaikh Moinuddin received his B.E. and M.Tech (Electrical), PhD on multi-phase inverter modeling and control, degrees in 1996, 1999 and 2009 respectively, from the Aligarh Muslim University, Aligarh, India. He is recipient of University Gold Medals for standing first in Electrical branch and in all branches of Engineering in 1996 B.E. exams. He has served Indian Air Force from 1971 to 1987. He is employed in the University Polytechnic, Aligarh Muslim University since 1987 where he is currently working as a Assistant Professor. His principal area of research interest is Power Electronics and Electric Drives.

Atif Iqbal received his B.Sc. and M.Sc. Engineering (Electrical) degrees in 1991 and 1996, respectively, from the Aligarh Muslim University, Aligarh, India and PhD in 2006 from Liverpool John Moores University, UK. He has been employed as Lecturer in the Department of Electrical Engineering, Aligarh Muslim University, Aligarh since 1991 and is working as Associate Professor in the same university. He is presently with Texas A&M University at Qatar on research assignment. He is recipient of Maulana Tufail Ahmad Gold Medal for standing first at B.Sc. Engg. Exams in 1991 at AMU, and EPSRC, Govt. Of UK, fellowship from 2002-2005 for pursuing PhD studies. His principal research interest is Modelling and Control of Power Electronics Converters & Drives.

Elmahdi M. Elsherif received his B. Sc. on Electrical and Electronics Engineering degree in 1987 from the Garyounes University, Benghazi, Libya, M.Sc. on Electrical Power Engineering and Management and PhD on load frequency control, in 1994 and 2002 respectively, from Dundee University Scotland. He is working as Head of Department of Electronics and Computer Engineering, Sebha University, Libya. His principal research interest is load flow analysis, control of automatic generation & drives.

Received, January 2010

Accepted, February 2010

Final acceptance in revised form, April 2010